LATTICE RELAXATIONS AROUND IMPURITIES IN METALS

P. H. Dederichs[1], N. Papanikolaou[1], N. Stefanou,[2] and R. Zeller[1]
[1] *Institut für Festkörperforschung, Forschungszentrum Jülich, D-52425 Jülich, Germany*
[2] *Section of Solid State Physics, University of Athens, Panepistimioupolis, GR-15784 Athens, Greece*

ABSTRACT

We review first-principle calculations of the size effect in dilute transition metal alloys. The calculations apply local density functional theory and a Green's function method based on the KKR-multiple scattering formalism. In each cell the full, anisotropic potential is included and the forces on the atoms are calculated by the Hellmann-Feynman theorem. The method is applied to predict the atomic positions around $d+sp$ impurities in Cu and Al. The results compare favorably with experimental data from extended X-ray-absorption fine-structure and lattice-parameter measurements.

1. INTRODUCTION

A point defect in a crystal, such as a vacancy or an impurity atom, presents not only a potential inhomogeneity, but also induces a displacement of the neighboring host atoms from their ideal lattice position. These displacements are in fact long ranged, varying with the inverse of the square of the distance from the impurity, and lead to a volume change of the crystal. Very complete information about this displacement field can be obtained by diffuse X-ray or neutron scattering, but unfortunately very few systems have been measured. Detailed information about many more systems has been obtained by extended X-ray-absorption fine-structure (EXAFS) measurements [1], yielding reliable data for the nearest neighbor shifts. In addition lattice parameter measurements [2, 3] are available for many systems, giving direct information about the volume changes induced by the impurities.

From the theoretical point of view the treatment of structural relaxation due to defects in crystals is a difficult task. In the past this problem has been mostly dealt with on a phenomenological basis, e.g. by applying models of lattice statics or continuum theory [4]. A reliable microscopic description of lattice relaxation effects based on first-principles electronic structure calculations requires very accurate total energies or forces and has mostly been attempted so far for simple metals and semiconductors on the basis of pseudopotential treatments. For instance, the pseudopotential supercell approach has been used to describe structural distortion in simple-metal [5] and semiconductor [6] systems. Lattice relaxation effects around defects in semiconductors have also been treated by the pseudopotential Green function method [7, 8].

In the paper we want to review the progress, which has been achieved recently, in calculating forces and lattice relaxations for transition metal systems [9, 10]. These calculations use the full-potential Korringa-Kohn-Rostoker (KKR) Green function method which offers an elegant and efficient framework for treating the impurity problem. In the following section we will shortly describe this method and details about the calculation of forces and lattice relaxations. In section 3 we will then present results obtained by this method for transition metal impurities and *sp* impurities in Cu. In section 4 similar results are given for the Al host. In both cases we discuss mostly $3d$ impurities and the connection between local moments and structural distortions. Moreover, we give also a detailed comparison with the experimental information obtained from EXAFS and lattice parameter measurements.

2. THEORETICAL METHOD

2.1. The Full Potential KKR Green Function Method

Within the framework of the KKR multiple scattering theory a crystalline solid is divided into non-overlapping space-filling cells around each atomic cite $\mathbf{R}^n$. The effective one-electron potential is written as a collection of individual potentials $V^n(\mathbf{r})$, which in each cell n are non-spherical and have a faceted cut-off structure. Using a site-centered expansion, the crystal Green function can be written in the form [11]

$$\begin{aligned} G(\mathbf{r}+\mathbf{R}^n,\mathbf{r}'+\mathbf{R}^{n'};E) &= \delta_{nn'}\, G_s^n(\mathbf{r}+\mathbf{R}^n,\mathbf{r}'+\mathbf{R}^{n'};E) \\ &\quad + \sum_{L,L'} R_L^n(\mathbf{r};E)\, G_{LL'}^{nn'}(E)\, R_{L'}^{n'}(\mathbf{r}';E) \end{aligned} \tag{1}$$

The vectors $\mathbf{r}$ and $\mathbf{r}'$ are restricted to the Wigner-Seitz cells around the atomic positions $\mathbf{R}^n$ and $\mathbf{R}^{n'}$, while $L=(\ell,m)$ denotes the angular momentum quantum numbers. G_s^n is the Green function for a single scattering potential in cell n in an otherwise free space. All multiple scattering contributions are contained in the second term through the so-called structural Green function $G_{LL'}^{nn'}(E)$. The wave function $R_L^n(\mathbf{r},E)$ is the solution of the single-potential-scattering problem with a spherical wave $j_\ell(\sqrt{E}r)Y_L(\hat{\mathbf{r}})$ of angular momentum L incident on a general potential $V^n(\mathbf{r})$, where $j_\ell(x)$ is a spherical Bessel function and $Y_L(\hat{\mathbf{r}})$ is a real spherical harmonic.

The electronic structure of a crystal with a localized perturbation, induced by the presence of a point defect for instance, can be obtained in two steps. We first calculate the ideal host Green function G^0 following a band structure calculation and obtain the host structural Green function $G^{0nn'}_{LL'}$ from (1). The Green function of the defect system can be then calculated in a second step from expansion (1), with the structural Green function given by the solution of the algebraic Dyson equation [11]

$$G^{nn'}_{LL'}(E) = G^{0nn'}_{LL'}(E) + \sum_{n'',L'',L'''} G^{0nn''}_{LL''}(E)\Delta t^{n''}_{L''L'''}(E)G^{n''n'}_{L'''L'}(E) \tag{2}$$

The summations in (2) extend only over those cells and angular momenta where the difference $\Delta t^n_{LL'}(E)$ between the t-matrices of the defect and the host system is significant. Equation (2) can be abbreviated in matrix form: $\mathcal{G} = \mathcal{G}^0 + \mathcal{G}^0\Delta t\mathcal{G}$.

For a general potential $V^n(\mathbf{r})$ the above t-matrices are given by

$$t^n_{LL'}(E) = \int d\mathbf{r}\; j_\ell(\sqrt{E}r)Y_L(\hat{\mathbf{r}})\; V^n(\mathbf{r})R^n_{L'}(\mathbf{r},E) \tag{3}$$

Since the potentials include non-spherical contributions, we expand both the wave function as well as the potential in real spherical harmonics [12]

$$R^n_L(\mathbf{r};E) = \sum_{L'} R^n_{L'L}(r;E)Y_{L'}(\hat{\mathbf{r}}) \tag{4}$$

$$V^n(\mathbf{r}) = \sum_L V^n_L(r)Y_L(\hat{\mathbf{r}}) \tag{5}$$

The non-spherical components of the potential couple the angular momentum channels and one is faced with the problem of a system of coupled radial equations. This is solved by an iterative procedure, starting from the solution of the spherical potential [12].

The division of the space into space-filling, non-overlapping cells is described by the shape functions $\Theta^n(\mathbf{r})$ which equal 1 inside cell n and vanish outside. The shape functions are expanded in real spherical harmonics

$$\Theta^n(\mathbf{r}) = \sum_L \Theta^n_L(r)Y_L(\hat{\mathbf{r}}) \tag{6}$$

The expansion coefficients $\Theta^n_L(\mathbf{r})$ are calculated with the algorithm of Stefanou *et al.* [13] following a semianalytical approach which can be used for any arbitrary Voronoi polyhedron.

The charge density is calculated from the Green function by integrating over all occupied energies. This integration can be performed efficiently by a contour integral in the complex energy plane [11, 12].

2.2. Dyson Equation for Displaced Atoms

Let us now suppose that we introduce a distortion in the crystal, displacing a number of atoms by $\mathbf{s}^n$ from their ideal lattice sites $\mathbf{R}^n$. The structural Green function

matrix $\mathcal{G}^0 = \{G^{0nn'}_{LL'}\}$ of the ideal host can be expanded around the shifted positions, with the help of the matrix transformation [14, 15]

$$\tilde{\mathcal{G}}^0 = \mathcal{U}\mathcal{G}^0\mathcal{U}^{-1} \tag{7}$$

The transformation matrix $\mathcal{U} = \{U_{LL'}(\mathbf{s}^n)\}$ is local in the site index and is given by

$$U_{LL'}(\mathbf{s}^n; E) = 4\pi \sum_{L''} i^{l+l''-l'} C_{LL'L''} j_{l''}(s^n\sqrt{E}) Y_{L''}(\hat{\mathbf{s}}^n) \tag{8}$$

where $C_{LL'L''} = \int d\hat{\mathbf{r}} Y_L(\hat{\mathbf{r}}) Y_{L'}(\hat{\mathbf{r}}) Y_{L''}(\hat{\mathbf{r}})$ are the Gaunt coefficients.

The defect structural Green functions $\mathcal{G}$, describing the real system with perturbed atoms located at the shifted positions $\mathbf{R}^n + \mathbf{s}^n$, is naturally expanded in the shifted coordinate system and related to the host structural Green function by the following Dyson equation

$$\mathcal{G} = \tilde{\mathcal{G}}^0 + \tilde{\mathcal{G}}^0(t - \tilde{t}^0)\mathcal{G} \tag{9}$$

where $\tilde{t}^0 = \mathcal{U}t^0\mathcal{U}^{-1}$ is the ideal host t-matrix in the expansion around the shifted position, and t is the defect t-matrix. We have used a tilde to denote quantities that are obtained using the coordinate system transformation.

A problem occurring in the transformation of the Green function $\mathcal{G}^0$ or the t-matrix t^0 is the angular momentum convergence. However for small shifts, to first order in the displacement, the only non-vanishing off-diagonal elements of the transformation matrix (8) are those with $|l - l'| = 1$ [15]. Therefore, for moderate lattice distortions, accurate calculations up to l_{max} can be done if angular momentum components up to $l_{max} + 1$ are included. The full-potential KKR Green function method has been found to give accurate, well-converged total energies and forces using a cut-off at $l_{max} = 3$. Therefore in the present calculation we use $l_{max} = 4$ in order to obtain reliable results.

2.3. Calculation of Forces and Lattice Relaxations

Calculation of interatomic forces is an important and difficult problem in electronic-structure calculations. According to the Hellmann-Feynman theorem the force on an atom is given by the electric field at the nuclear position due to all electrons and all other nuclei. The application of this theorem is however severely limited, since it requires a full-potential treatment of the core electrons. This problem can be overcome by making a spherical ansatz $\rho^n_c(r)$ for the core density entering in the total energy expression. The force is then calculated as the derivative of the total energy with respect to the nuclear position assuming that the Kohn-Sham equations are solved exactly for the valence electrons only. The resulting expression for the force $\mathbf{F}^n$ on the atom $\mathbf{R}^n$ is given by [16, 17]

$$\mathbf{F}^n = Z^n \partial_{\mathbf{r}} V^n_C(\mathbf{r})|_{\mathbf{r}=0} - \int d^3r \rho^n_c(r) \partial_{\mathbf{r}} V^n(\mathbf{r}) \tag{10}$$

where V^n_C is the Coulomb part of the effective one-electron potential in cell n due to all electrons and all other nuclei. Clearly the first term is the force on the nucleus,

evaluated with spherical core charge densities and the second term is the force on the core electrons. Since V^n is the effective Kohn-Sham potential, the latter term includes both electrostatic and exchange-correlation contributions arising from the exchange and correlation between core and valence electrons.

Using the angular momentum expansion (5) for the potential, one finally obtains for the $i = x, y, z$ component of the force on atom n

$$F_i^n = Z^n \sqrt{\frac{3}{4\pi}} \left. \frac{V_{C;1i}^n(r)}{r} \right|_{r=0} - \sqrt{\frac{4\pi}{3}} \int dr \; \rho_c^n(r) \frac{\partial}{\partial r} \left(r^2 V_{1i}^n(r) \right) \tag{11}$$

As we see from this result, within the KKR Green function method the force calculation requires no additional effort, since the force is readily calculated from the $l = 1$ component of the potential which is anyhow evaluated self-consistently. Furthermore one can show that Pulay corrections to the Hellmann-Feynman force formula (10), arising from the finiteness of the basis used in the calculations, vanish within the full potential KKR formalism [17].

Knowing the forces, the determination of the displacements $\mathbf{s}^n$ describing the equilibrium structure is another non-trivial task. In order to accelerate convergence we use here a lattice statics procedure known as Kanzaki method [4, 9]. This requires the calculation of the Kanzaki forces

$$\mathbf{F}_K^n \; = \; \mathbf{F}^n - \sum_{n'} \Delta \underline{\underline{\phi}}^{nn'} \mathbf{s}^{n'} \tag{12}$$

where $\mathbf{F}^n$ are the Hellmann-Feynman forces (10) and $\Delta\underline{\underline{\phi}}$ are the changes of the Born-von-Karman coupling parameters in the vicinity of the defect, being estimated from calculations with given $\mathbf{s}^{n'}$. Within lattice statics the displacements are then determined by

$$\mathbf{s}^n \; = \; \sum_{n'} \underline{\underline{G}}^{nn'} \; \mathbf{F}_K^{n'}(\mathbf{s}) \tag{13}$$

where $\underline{\underline{G}}^{nn'}$ is the lattice Green function of the ideal harmonic crystal (without the defect). In this way a new displacement pattern $\mathbf{s}^n$ for all atoms around the impurity is generated which serves as input for another electronic-structure and force calculation, etc. In practical cases only one or two self-consistency cycles are needed.

3. LATTICE RELAXATIONS IN Cu

3.1. Consistency of Force and Total Energy

In order to check the reliability of the calculated forces, we allow only a relaxation of the first neighbors of the impurity, by fixing the more distant ones at their regular positions. The equilibrium positions can then either be calculated from the minimum of the total energy, or from the condition of vanishing forces. The good agreement between results represents a stringent test of the accuracy of the force calculation.

3.2. Importance of Semicore States

In the force formula (10) the role of the core and valence electrons is very different, since the core charge density is assumed to be spherically symmetric, while the valence charge density is calculated exactly. For the semicore states the question therefore arises, if they are sufficiently localized to be treated as core states. For the $3d$-impurities in Cu, we find that this is not the case for the 3p semicore states. For instance, for a Ti impurity the force on the neighboring Cu atoms is about 50 % too large, if the semicore charge density of the impurity is considered as spherical. Thus for the early transition metal impurities in Cu the 3p semicore states have to be treated as valence states, since they give an important binding contribution to the forces.

3.3. Displacements of Nearest Neighbors

For the case of $3d$ impurities in Cu, Fig. 1 shows the displacements of the NN Cu atoms calculated by the Kanzaki procedure. Also included are experimental values form EXAFS measurements by Scheuer and Lengeler [1] which agree with the calculated results within the experimental uncertainty. In most cases the Cu lattice is dilated by the impurities, except for the cases of Fe, Co or Ni impurities.

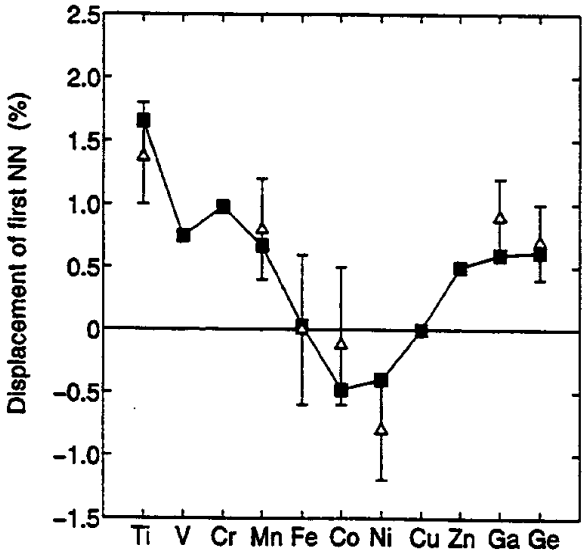

Figure 1. Relative displacements of the nearest neighbor Cu atoms (with respect to the n.n. distance) for 3d and 4sp impurities in Cu. The triangles with error bars give the results of EXAFS measurements [1].

Since the 3d impurities in Cu are magnetic, it is interesting to see how the local moments are affected by the lattice displacement. We find that this influence is vanishingly small. Our calculation gives for the local moments of V, Cr, Mn, Fe, and

Co impurities: 0.98 (0.85), 2.96 (2.91), 3.42 (3.39), 2.53 (2.53), and 0.96 (1.01) Bohr magnetons, respectively, in the relaxed (unrelaxed) geometry. These results show that outward relaxations slightly increase the moments (V, Cr, and Mn), while inward relaxations lead to a small decrease of the magnetic moment (Co). For Fe there is no relaxation of the first NN so that, in this case, there is no moment change. This vanishingly small influence of the local lattice distortion on the impurity moments can be understood, if we compare the spin-polarization energies of the impurities [18] with lattice relaxation energies. While the relaxation energies in the whole series from V to Ge are smaller than 0.03 eV, the spin-polarization energies of the magnetic impurities are huge, e.g. 0.7 eV for Mn, 0.36 eV for Fe and 0.39 eV for Cr. Therefore in Cu the local moments are very stable and practically not affected by the relaxations.

3.4. Induced Volume Change

For a statistical distribution of many point defects the lattice expansion or compression due to the individual defects results in a change of the crystal volume. In the case of cubic metals the volume change due to a single defect is given by the first moment of the Kanzaki forces [4]

$$\Delta V = V - V_0 = \frac{1}{3K} \sum_n \mathbf{F}_K^n \cdot \mathbf{R}^n \tag{14}$$

where V and V_0 are the atomic volumes of the defect system and the ideal host, respectively, and K is the bulk modulus of pure Cu: $K = 1.55$ Mbar. As an example we present in Fig. 2 the calculated relative volume changes $\Delta V/V_0$ for $4d$ impurities in Cu, together with the experimental data as obtained from lattice-parameter measurements [2, 3]. For cubic crystals the volume change is related to the change of the lattice parameter by $\Delta V/V_0 = 3\Delta a/a_0$. The agreement with the experiment is good.

The relative sizes of the nearest neighbor displacements and the volume changes can be estimating from a simple elasticity model. Assuming that the asymptotic displacement field, varying as $1/r^2$ in elasticity theory (r = distance from impurity), is already valid at the nearest neighbor sites, the volume change of a sphere with radius equal to the nearest neighbor distance a_{NN} is given by $\Delta V \cong 4\pi a_{NN}^2 s_{NN}$, where s_{NN} is the nearest neighbor displacement. Inserting the values $a_{NN} = a/\sqrt{2}$, $V_0 = a^3/4$ for the fcc lattice and correcting for the image expansion [4] we obtain in this model: $\Delta V/V_0 \approx 27 s_{NN}/a_{NN}$. The simple model explains the similarity between the ΔV and s_{NN} curves found in the calculation. Also the prefactor 27 is reasonable.

The dashed line in Fig. 2 refers to the volume expansion as estimated by Vegard's law. This indeed shows the qualitative trends as observed for the sp and early 3d impurities. However the bump in the curve for Fe, Mn and Cr impurities cannot be explained in this way. It results from the large local moments of the impurities, leading to a sizeable magneto-volume expansion. The same effect can also be seen for the displacements in Fig. 1.

4. LATTICE RELAXATIONS IN Al

Al is a three-valent simple metal with a rather high electron density. Nevertheless its lattice constant is about 10 % larger than the one of Cu. Both facts are important for understanding the defect relaxations in Al as compared to Cu.

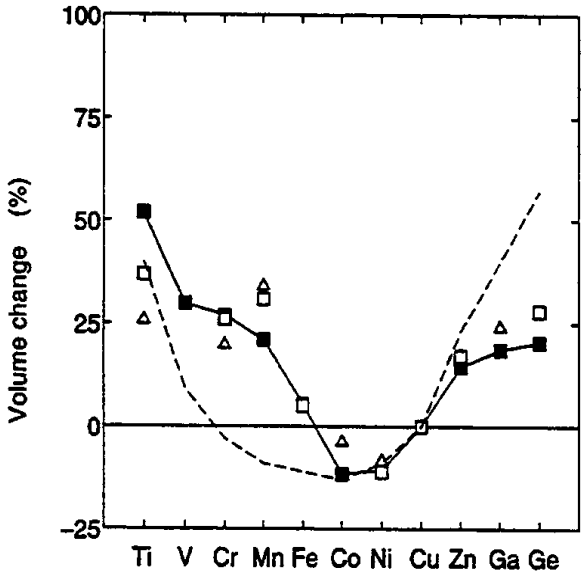

Figure 2. Volume changes (in units of the elementary volume) due to 3d and 4sp impurities in Cu. The squares and triangles denote experimental values from lattice parameter measurements [2, 3]. The dashed line is obtained using Vegard's law.

Fig. 3 shows the predicted displacements of the first nearest neighbors for $3d$ and $4sp$ impurities in Al. The results are in good agreement with the available experimental data from EXAFS measurements [1]. Upon alloying with $3d$ elements the Al lattice contracts. Across the $3d$ series the resulting displacements show a parabolic behavior with a minimum at Fe, while in the case of $4sp$ impurities we find only very small distortions. As compared to Cu the displacements in Al are much larger, which can only partially be explained by the differences between the host lattice constants. For instance, in Cu the difference between the NN relaxations of Co and Ge is about 1 %, while in Al this difference amounts to 4.5 %. Clearly the different bonding in both hosts is very important. In particular the formation of the strong and compact bonds between the impurity d- and Al p-electrons leads to the large contraction in the $3d$ series. As a consequence the relaxation energies, varying quadratically with the distortions, are very large (Fig. 4). For instance, for Co and Fe in Al, these amount to 0.42 and 0.44 eV which is more than an order of magnitude larger than the corresponding values in Cu.

The strong d-p hybridization between the impurity d-states and the Al p-electrons dramatically affects the local moments. In the unrelaxed configuration only Cr, Mn and

Fe impurities are magnetic, with moments of 2.2, 2.6 and 1.7 μ_B. The corresponding spin-polarization energies are shown in Fig. 4. They are considerably smaller than the spin polarization energies in Cu, which amount to e.g. 0.7 eV for Mn and 0.36 eV for Fe. More important is that these energies are smaller than the energies being gained in Al by lattice relaxations. The corresponding relaxation energies are also shown in Fig. 4. Since the inward relaxation increases the *p-d* hybridization, this has the tendency to strongly reduce the local moments. From energetic point of view the large gain in relaxation energy can overcome the loss of spin-polarization energy. For the equilibrium configuration we find a moment of 0.7 μ_B for Cr, 1.3 μ_B for Mn and a vanishing moment for Fe. Experimentally Cr and Mn in Al are spin-fluctuation systems with Kondo-temperatures of 500 K and 1500 K [19], being in qualitative agreement with our results. The result for Fe is in accordance with the experimental finding that Fe is non-magnetic in Al. In fact in the calculation the Fe-moment vanishes already at a relaxation of 2.8 %, being appreciably smaller than the equilibrium value of 4.2 %.

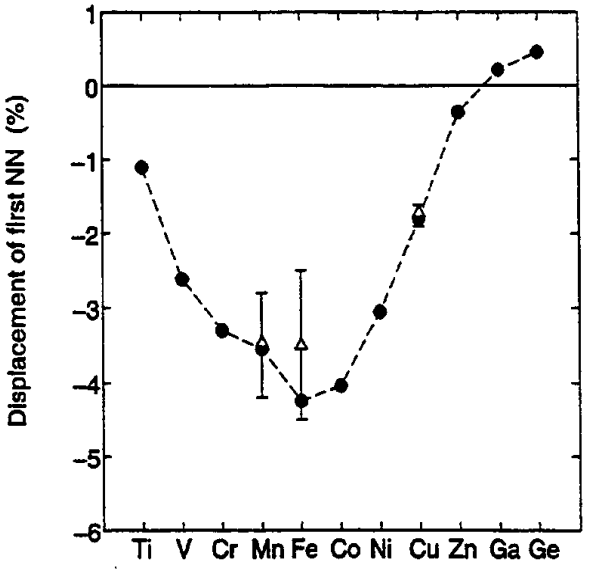

Figure 3. Relative displacements of the n.n. Al atoms due to 3d and 4sp impurities in Al. The triangles denote results form EXAFS measurements [1].

Thus when we compare the magnetic and structural properties of $3d$ impurities in Cu and Al, we find a very different behavior. In Cu the spin-polarization energies are large and the relaxation energies very small, typically 0.03 eV. Therefore the local moments are very stable and practically not affected by the relaxations. On the other hand the relaxations themselves are small, but depend strongly on magnetism. In Al we are in the opposite limit of large relaxation energies and small spin polarization energies (Fig. 4). Therefore the relaxations are large, with only a small magnetic

anomaly appearing for the Mn impurity, while the moments are relatively small and strongly depend on relaxations.

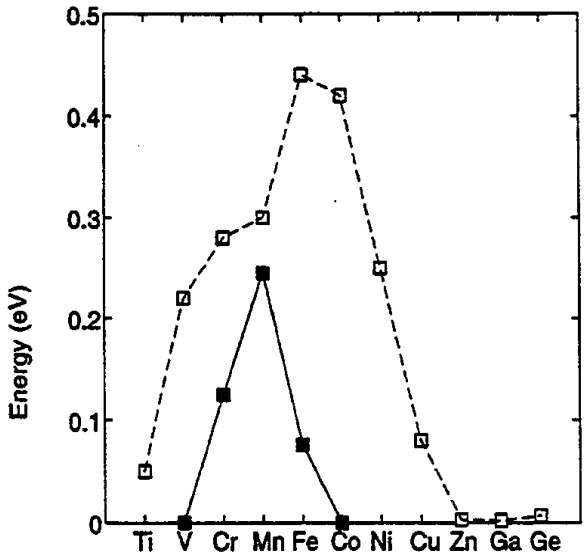

Figure 4. Lattice relaxation energies (dashed line) and spin polarization energies (full line, for the unrelaxed configuration) for 3d and 4sp impurities in Al.

5. SUMMARY

We have presented an *ab initio* method to calculate lattice distortions around point defects in metals. The method was applied to $3d$ and $4sp$ impurities in Cu and Al. We have shown that the full potential KKR Green function method allows an accurate and easy calculation of forces, since Pulay-type corrections to the Hellmann-Feynman force vanish. The results for the NN shifts and the volume changes induced by the defect are in very good agreement with data from EXAFS and lattice parameter measurements. We believe that the present method can be successfully applied to many other structural or dynamical properties of solids, e.g. relaxations of ideal surfaces or of surfaces with adsorbate atoms, phonons of transition metals or of transition metal surfaces etc.

References

[1] U. Scheuer and B. Lengeler, Phys. Rev. B 44, 9883 (1991)

[2] H. W. King, J. Mat. Sci. 1, 79 (1966)

[3] W. B. Pearson, *A Handbook of Lattice Spacings and Structures of Metals and Alloys*, Vol. 1 (Pergamon Press, London, 1958), p. 570; Vol. 2 (Pergamon Press, Oxford, 1967) p. 868

[4] G. Leibfried and N. Breuer, *Point Defects in Metals I* (Springer-Verlag, Berlin, 1978)

[5] R. Pawellek, M. Fähnle, C. Elsässer, K. M. Ho and C. T. Chan, J. Phys.: Condens. Matter **3**, 2451 (1991); R. Benedek, L. H. Yang, C. Woodward, B. I. Min, Phys. Rev. B **45**, 2607 (1992)

[6] Y. Bar-Yam and J. D. Joannopoulos, Phys. Rev. Lett. **52**, 1129 (1984); Phys. Rev. B **30**, 1844 (1984)

[7] M. Scheffler, J. P. Vigneron, and G. B. Bachelet, Phys. Rev. Lett. **49**, 1765 (1982); Phys. Rev. B **31**, 6541 (1985); M. Scheffler, Physica **146B**, 176 (1987)

[8] G. A. Baraff and M. Schlüter, Phys. Rev. B **30**, 1853 (1984); Phys. Rev. Lett. **55**, 1327 (1985)

[9] N. Papanikolaou, R. Zeller, P. H. Dederichs and N. Stefanou, Phys. Rev. B **55**, 4157 (1997)

[10] N. Papanikolaou, R. Zeller, P. H. Dederichs and N. Stefanou, Comp. Mat. Science (accepted)

[11] P. J. Braspenning, R. Zeller, A. Lodder, and P. H. Dederichs, Phys. Rev. B **29**, 703 (1984)

[12] P. H. Dederichs, B. Drittler, and R. Zeller, Mat. Res. Soc. Symp. Proc. **253**, 185 (1992)

[13] N. Stefanou, H. Akai, and R. Zeller, Comput. Phys. Commun. **60**, 231 (1990); N. Stefanou and R. Zeller, J. Phys.: Condens. Matter **3**, 7599 (1991)

[14] A. Lodder, J. Phys. F **6**, 1885 (1976)

[15] N. Stefanou, P. J. Braspenning, R. Zeller, and P. H. Dederichs, Phys. Rev. B **36**, 6372 (1987)

[16] J. Harris, R. O. Jones, and J. E. Müller, J. Chem. Phys. **75**(8), 3904 (1981)

[17] K. Abraham, Diploma thesis, RWTH Aachen (1991) (unpublished)

[18] P. H. Dederichs, T. Hoshino, B. Drittler, K. Abraham, and R. Zeller, Physica B **172**, 203 (1991)

[19] F.J. Kedves, M. Hordos, and L. Gergely, Solid State Commun. **11**, 1067 (1972); E. Babic, P.J. Ford, C. Rizzuto, and E. Salamoni, J. Low Temp. **8**, 219 (1972)